Electronic Supplementary Material (ESI) for Catalysis Science & Technology.
This journal is © The Royal Society of Chemistry 2020

Supporting Information

Exploring Direct and Hydrogen-Assisted CO Activation on Iridium Surfaces – Surface Dependent Activity

Chunli Liu,[a,b,c] Ling Zhu,[a,b,c] Xiaodong Wen,[a,b] Yong Yang [a,b] Yong-Wang Li,[a,b] Haijun Jiao[a,d]*

a) State Key Laboratory of Coal Conversion, Institute of Coal Chemistry, Chinese Academy of Sciences, Taiyuan, 030001, China; b) National Energy Center for Coal to Liquids, Synfuels China Co., Ltd, Huairou District, Beijing, 101400, China; c) University of Chinese Academy of Sciences, No. 19A Yuquan Road, Beijing, 100049, China; d) Leibniz-Institut für Katalyse e.V. an der Universität Rostock, Albert-Einstein Strasse 29a, 18059 Rostock, Germany. E-mail: haijun.jiao@catalysis.de

Contents

Sum of Bond valences (SBV)

The concept of bond valence, developed from the concept of bond number by Pauling,[1] has been widely applied in solid-state chemistry.[2] SBV can measure the relative strength of the various bonds quantitatively.[3,4] Bond valence is most commonly calculated by the empirical equation (1),[5] where r_0 is the bond valence parameter, r_{ij} is the bond length between the two atoms i and j, and B is a universal constant equal to 0.37 Å. In this work, r_0 = 1.60 Å is used for the Ir–H bond; r_0 = 1.70 Å is used for the Ir–C bond; r_0 = 1.916 Å is used for the Ir–O bond.[6]

$$SBV_{ij} = \sum exp^{[0]}\left(\frac{r_0 - r_{ij}}{B}\right) \qquad (1)$$

Vibrational energy contribution

In details, when we consider the contribution of the vibrational at the experimental conditions, the standard molar vibrational internal energy contribution is calculated as Equation (2)[7]:

$$U_{vib}^{\circ} = RT\sum_i \frac{h\nu_i/K_BT}{e^{h^{\nu}i/K_BT} - 1} \qquad (2)$$

Where *h* is Planck's constant, K_B is Boltzmann constant and *R* is the gas constant. The standard molar vibrational entropy is given

$$S_{vib}^{\circ} = R\sum\left[\frac{h\nu_i/K_BT}{h\nu_i/K_BT} - ln\left(1 - e^{-h\nu_i/K_BT}\right)\right] \qquad (3)$$

by Equation (3):

Overall, when the free energy corrections are added together, the standard molar Gibbs free energy (*G)* can be written as Equation (4):

$$G = E + \gamma RT\left(1 + ln\frac{P}{P^{\square}}\right) + U_{vib}^{\circ} - TS_{vib}^{\circ} \qquad (4)$$

Where *E* is represents the total energies from the VASP calculation (with ZPE correction). If the molecule is gaseous, then 1 is chosen as the value of γ and 0 is selected for adsorbed species.

Table S1. Barriers (E_a, eV) of CO direct dissociation and H-assisted dissociation on the different surfaces, and the distances of C–O bonding at the transition states are shown in the bracket.

Reaction Step	(111)		(100)		Ir(110)		Ir(210)		Ir(311)		Ir(221)	
	E_a ($d_{C-O/H}$)	E_r	E_a ($d_{C-O/H}$)	E_r	E_a ($d_{C-O/H}$)	E_r	E_a ($d_{C-O/H}$)	E_r	E_a ($d_{C-O/H}$)	E_r	E_a ($d_{C-O/H}$)	E_r
CO*→C*+O*	3.17 (1.84)	1.52	2.29 (1.90)	0.58	2.65 (1.86)	1.11	2.56 (1.88)	0.80	2.40 (2.01)	1.18	2.67 (1.85)	1.13
CO*+H*→COH* (R1)	1.69 (1.34)	0.66	1.60 (1.23)	0.95	2.01 (1.30)	1.24	1.82 (1.23)	1.35	2.13 (1.27)	1.30	2.28 (1.32)	1.08
CO*+H*→HCO* (R2)	1.58 (1.21)	1.10	1.59 (1.36)	0.97	1.35 (1.18)	0.98	1.34 (1.21)	0.47	1.74 (1.17)	1.17	1.50 (1.18)	1.01
COH*→C*+OH* (R3)	2.29 (1.87)	1.00	1.21 (1.98)	–0.24	1.31 (1.95)	0.18	1.07 (1.94)	–0.41	1.13 (1.97)	0.11	1.62 (1.95)	0.40
COH*+H*→HCOH* (R4)	0.96 (1.36)	0.83	1.08 (1.27)	0.77	0.64 (1.33)	0.41	1.35 (1.67)	0.58	0.84 (1.33)	0.53	0.83 (1.30)	0.40
HCO*+H*→HCOH* (R5)	0.94 (1.33)	0.39	1.15 (1.49)	0.75	1.05 (1.39)	0.67	1.08 (1.40)	1.46	1.27 (1.39)	0.65	1.09 (1.39)	0.47
HCO*+H*→H_2CO* (R6)	0.88 (1.22)	0.66	1.17 (1.16)	1.11	0.85 (1.19)	0.66	0.96 (1.16)	1.41	0.97 (1.22)	0.71	0.76 (1.22)	0.62
HCO*→HC*+O* (R7)	1.58 (2.09)	–0.12	0.60 (2.03)	–0.31	1.78 (2.17)	0.64	1.09 (2.03)	0.63	1.69 (2.09)	–0.15	2.12 (2.07)	–0.27
HCOH*→HC*+OH* (R8)	0.47 (2.09)	–0.29	0.40 (1.78)	–0.93	0.87 (1.87)	–0.31	0.74 (1.94)	–0.81	1.04 (1.89)	–0.54	0.90 (2.14)	–0.30
HCOH*+H*→H_2COH* (R9)	0.54 (1.42)	0.22	1.19 (1.22)	0.76	1.14 (1.65)	0.34	0.85 (1.44)	0.50	1.22 (1.24)	0.57	0.99 (1.16)	0.66
H_2CO*+H*→H_2COH* (R10)	0.48 (1.48)	–0.05	0.71 (1.41)	0.40	1.23 (1.46)	0.35	0.93 (1.40)	0.56	1.46 (1.49)	0.51	0.84 (1.41)	0.51
H_2CO*+H*→H_3CO* (R11)	0.54 (1.63)	0.22	1.04 (1.89)	0.45	0.72 (1.47)	0.56	0.94 (2.14)	0.57	0.83 (1.57)	0.62	0.89 (1.52)	0.67
H_2CO*→H_2C*+O* (R12)	1.06 (2.33)	–0.14	1.15 (2.35)	–0.47	0.99 (2.37)	–0.49	0.68 (2.05)	–0.30	1.03 (2.19)	–0.56	1.09 (2.28)	–0.51
H_2COH*→H_2C*+OH* (R13)	0.96 (2.83)	0.14	0.63 (2.70)	–0.72	0.50 (2.23)	–0.51	0.26 (1.99)	–0.60	0.48 (2.21)	–0.78	0.45 (2.29)	–0.64
H_2COH*+H*→H_3COH* (R14)	0.78 (1.51)	0.06	1.11 (1.41)	0.63	0.92 (1.38)	0.49	0.89 (1.43)	0.58	1.16 (1.39)	0.77	0.91 (1.63)	0.49
H_3CO*+H*→H_3COH* (R15)	0.48 (1.41)	–0.21	0.99 (1.48)	0.58	1.08 (1.40)	0.29	1.04 (1.37)	0.57	1.08 (1.43)	0.66	0.77 (1.47)	0.33
H_3CO*→H_3C*+O* (R16)	1.59 (2.08)	–0.34	1.68 (2.16)	–0.31	1.66 (1.82)	–0.67	--	–0.51	1.41 (1.90)	–0.62	1.31 (1.93)	–0.61
H_3COH*→H_3C*+OH* (R17)	1.29 (2.06)	0.12	1.50 (2.05)	–0.73	1.54 (2.16)	–0.64	1.37 (2.21)	–0.93	--	–1.05	1.44 (1.93)	–0.57

Table S2. The barrier difference between the reaction energies with ($E_{a\text{-}v}$, eV) and without (E_a, eV) vibrational energy contribution of CO direct dissociation and H-assisted dissociation on the different surfaces

Reaction Step	(111)			(100)			Ir(110)			Ir(210)			Ir(311)			Ir(221)		
	E_a	$E_{a\text{-}v}$	ΔE_a	E_a	$E_{a\text{-}v}$	ΔE_a	E_a	$E_{a\text{-}v}$	ΔE_a	E_a	$E_{a\text{-}v}$	ΔE_a	E_a	$E_{a\text{-}v}$	ΔE_a	E_a	$E_{a\text{-}v}$	ΔE_a
CO*→C*+O*	3.17	3.11	–0.06	2.29	2.26	–0.03	2.65	2.60	–0.05	2.56	2.51	–0.05	2.40	2.40	0.00	2.67	2.62	–0.05
CO*+H*→COH* (R1)	1.69	1.68	0.01	1.60	1.60	0.00	2.01	1.97	–0.04	1.82	1.80	–0.02	2.13	2.16	0.03	2.28	2.25	–0.03
CO*+H*→HCO* (R2)	1.58	1.59	0.01	1.59	1.63	0.04	1.35	1.37	0.02	1.34	1.36	0.02	1.74	1.78	0.04	1.50	1.51	0.01
COH*→C*+OH* (R3)	2.29	2.30	0.01	1.21	1.21	0.00	1.31	1.33	0.02	1.07	1.05	–0.02	1.13	1.07	–0.06	1.62	1.64	0.02
COH*+H*→HCOH* (R4)	0.96	0.97	0.01	1.08	1.14	0.06	0.64	0.68	0.04	1.35	1.35	0.00	0.84	0.85	0.01	0.83	0.89	0.06
HCO*+H*→HCOH* (R5)	0.94	1.03	0.09	1.15	1.23	0.08	1.05	1.05	0.00	1.08	1.08	0.00	1.27	1.30	0.03	1.09	1.09	0.00
HCO*+H*→H_2CO* (R6)	0.88	1.00	0.12	1.17	1.24	0.07	0.85	0.88	0.03	0.96	1.00	0.04	0.97	0.99	0.02	0.76	0.78	0.02
HCO*→HC*+O* (R7)	1.58	1.71	0.13	0.60	0.62	0.02	1.78	1.81	0.03	1.09	1.10	0.01	1.69	1.77	0.08	2.12	2.18	0.06
HCOH*→HC*+OH* (R8)	0.47	0.50	0.03	0.40	0.36	–0.04	0.87	0.86	–0.01	0.74	0.74	0.00	1.04	1.08	0.04	0.90	0.92	0.02
HCOH*+H*→H_2COH* (R9)	0.54	0.54	0.00	1.19	1.23	0.04	1.14	1.19	0.05	0.85	0.90	0.05	1.22	1.24	0.02	0.99	1.05	0.06
H_2CO*+H*→H_2COH* (R10)	0.48	0.50	0.02	0.71	0.71	0.00	1.23	1.27	0.04	0.93	0.94	0.01	1.46	1.49	0.03	0.84	0.86	0.02
H_2CO*+H*→H_3CO* (R11)	0.54	0.54	0.00	1.04	1.07	0.03	0.72	0.77	0.05	0.94	0.93	–0.01	0.83	0.87	0.04	0.89	0.92	0.03
H_2CO*→H_2C*+O* (R12)	1.06	1.06	0.00	1.15	1.15	0.00	0.99	1.03	0.04	0.68	0.70	0.02	1.03	1.07	0.04	1.09	1.13	0.04
H_2COH*→H_2C*+OH* (R13)	0.96	0.94	–0.02	0.63	0.59	–0.04	0.50	0.49	–0.01	0.26	0.27	0.01	0.48	0.58	0.10	0.45	0.45	0.00
H_2COH*+H*→H_3COH* (R14)	0.78	0.81	0.03	1.11	1.10	–0.01	0.92	0.95	0.03	0.89	0.89	0.00	1.16	1.25	0.09	0.91	0.90	–0.01
H_3CO*+H*→H_3COH* (R15)	0.48	0.49	0.01	0.99	1.04	0.05	1.08	1.09	0.01	1.04	1.05	0.01	1.08	1.15	0.07	0.77	0.81	0.04
H_3CO*→H_3C*+O* (R16)	1.59	1.58	–0.01	1.68	1.65	–0.03	1.66	1.67	0.01	--	--	--	1.41	1.41	0.00	1.31	1.30	–0.01
H_3COH*→H_3C*+OH* (R17)	1.29	1.27	–0.02	1.50	1.49	–0.01	1.54	1.56	0.02	1.37	1.39	0.02	--	--	--	1.44	1.39	–0.05

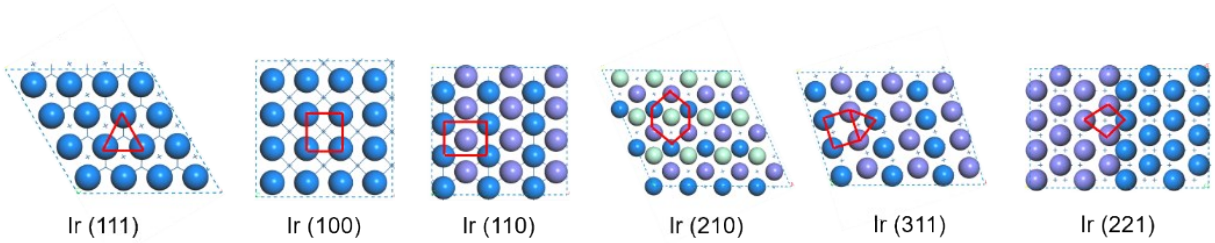

Figure S1. High coordination site for CO dissociation on the Ir(111), Ir(100), Ir(110), Ir(210), Ir(311) and Ir(221) surfaces

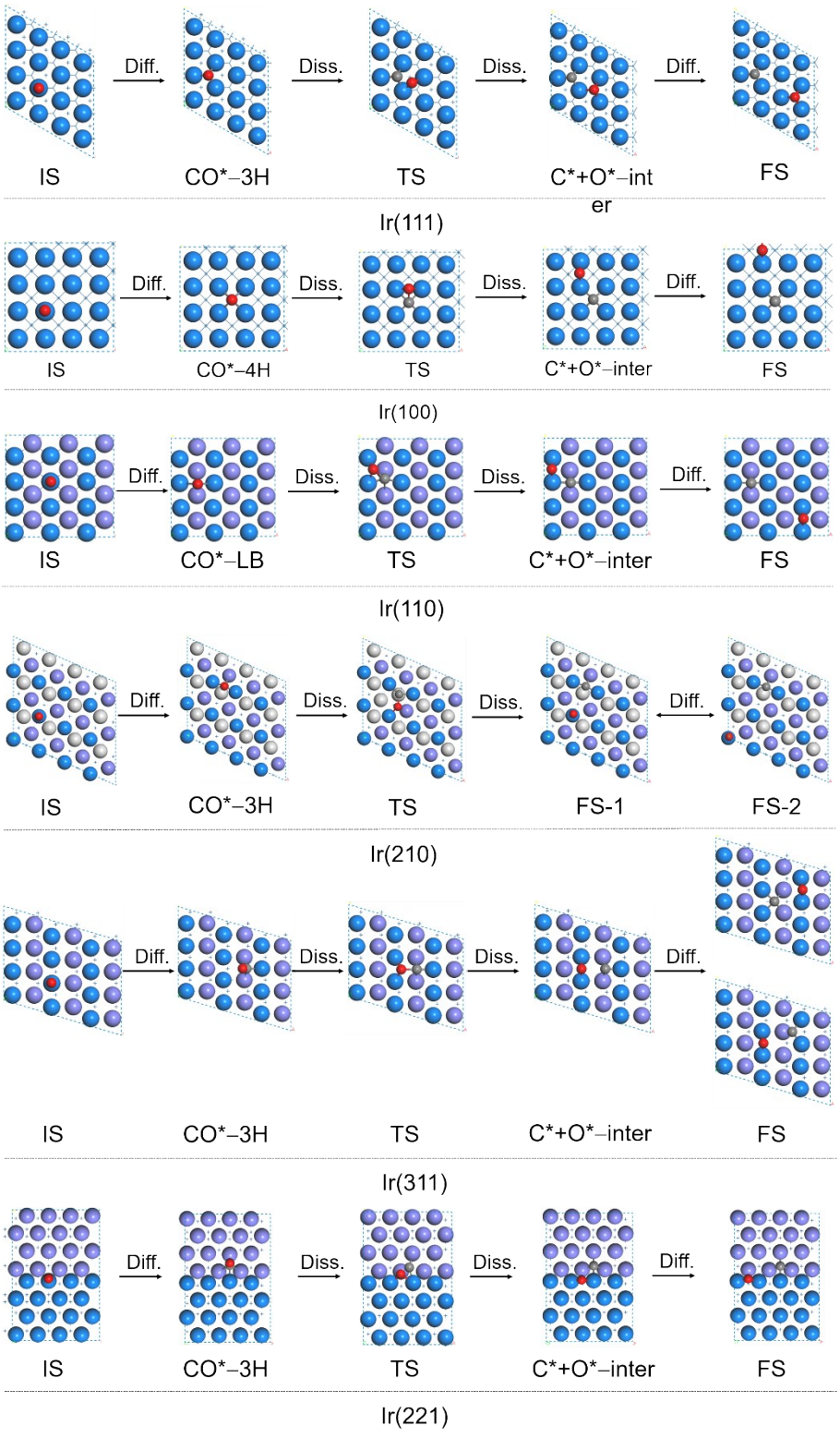

Figure S2. Route of direct CO dissociation on the Ir(111), Ir(100), Ir(110), Ir(210), Ir(311) and Ir(221) surfaces

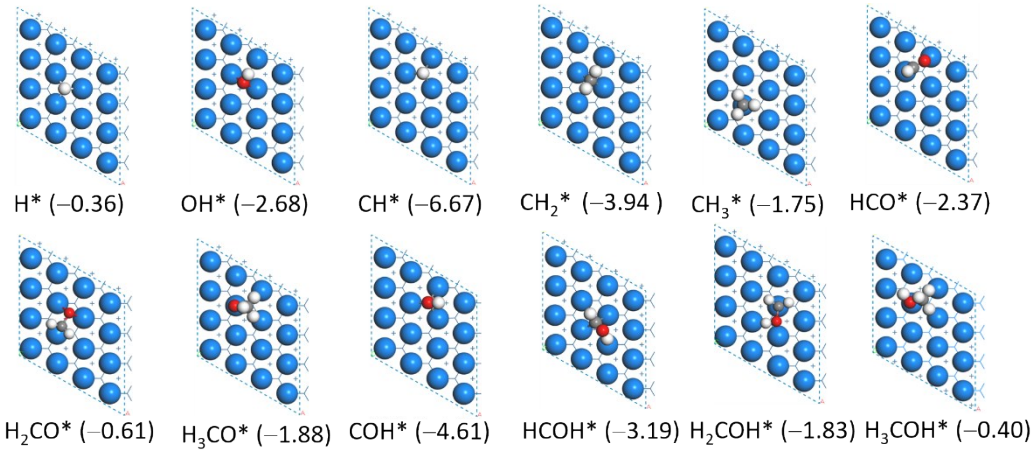

Figure S3 Top views of the most stable adsorption configuration with adsorption energy (E_{ads}, eV) for H, OH, CH, CH_2, CH_3, CHO, CH_2O, CH_3O, COH, CHOH, CH_2OH, CH_3OH on the Ir(111) surface

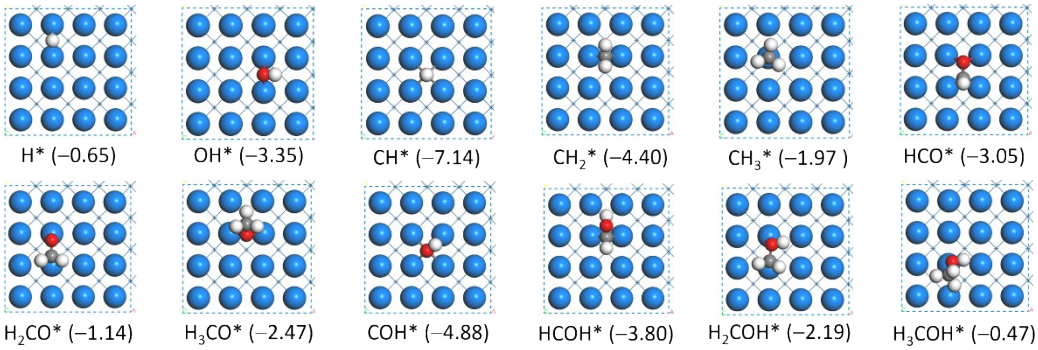

Figure S4 Top views of the most stable adsorption configuration with adsorption energy (E_{ads}, eV) for H, OH, CH, CH_2, CH_3, CHO, CH_2O, CH_3O, COH, CHOH, CH_2OH, CH_3OH on the Ir(100) surface

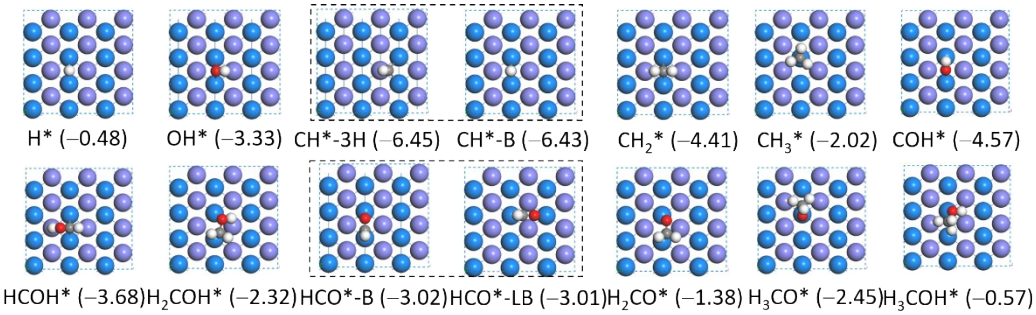

Figure S5 Top views of the most stable adsorption configuration with adsorption energy (E_{ads}, eV) for H, OH, CH, CH_2, CH_3, CHO, CH_2O, CH_3O, COH, CHOH, CH_2OH, CH_3OH on the Ir(110) surface

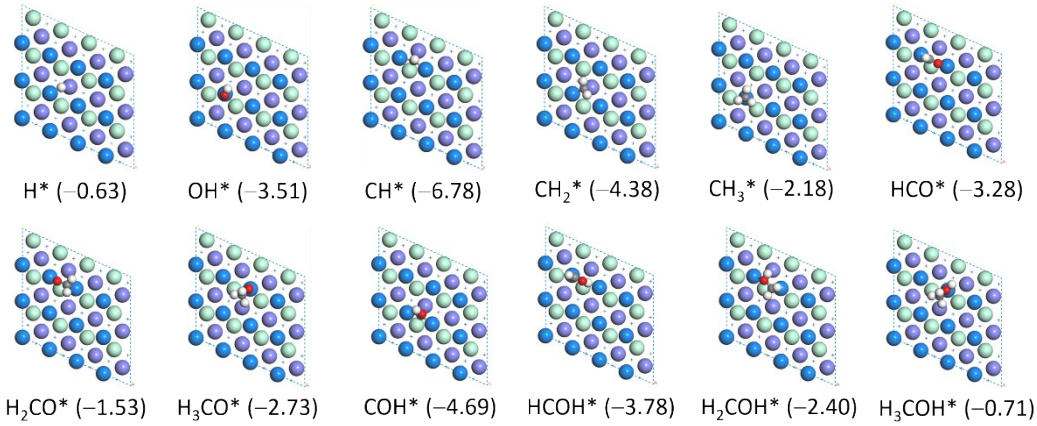

Figure S6 Top views of the most stable adsorption configuration with adsorption energy (E_{ads}, eV) for H, OH, CH, CH_2, CH_3, CHO, CH_2O, CH_3O, COH, CHOH, CH_2OH, CH_3OH on the Ir(210) surface

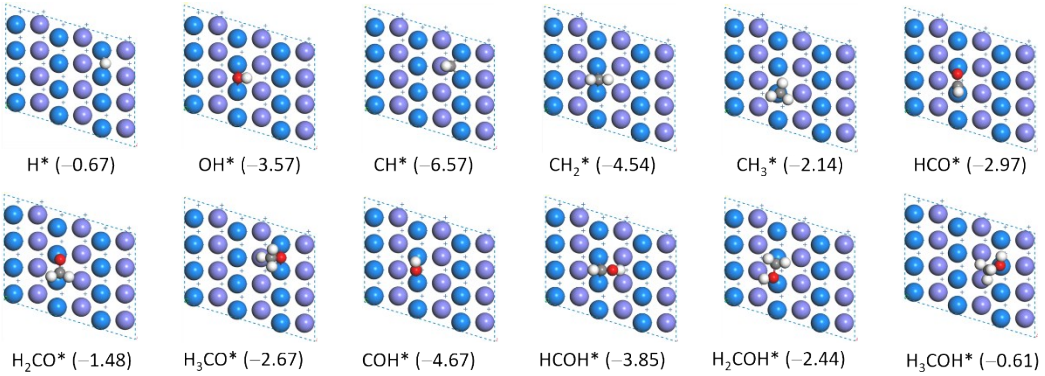

Figure S7 Top views of the most stable adsorption configuration with adsorption energy (E_{ads}, eV) for H, OH, CH, CH_2, CH_3, CHO, CH_2O, CH_3O, COH, CHOH, CH_2OH, CH_3OH on the Ir(311) surface

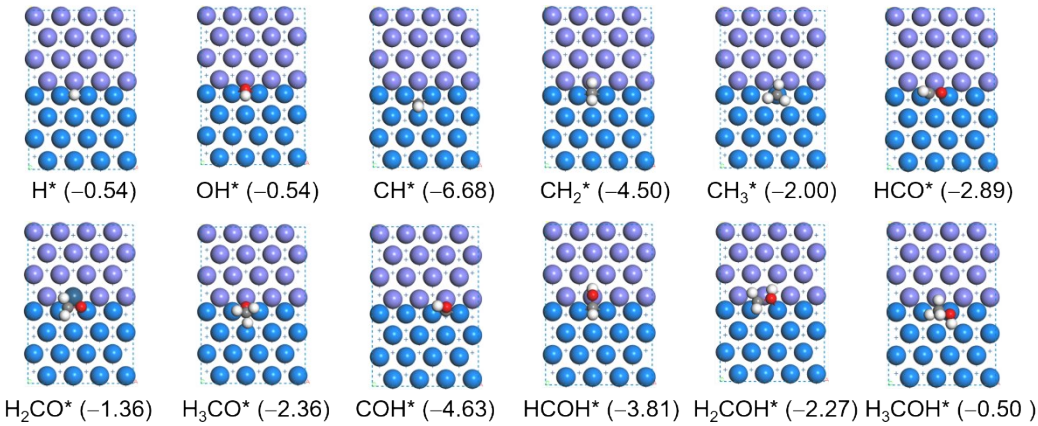

Figure S8 Top views of the most stable adsorption configuration with adsorption energy (E_{ads}, eV) for H, OH, CH, CH_2, CH_3, CHO, CH_2O, CH_3O, COH, CHOH, CH_2OH, CH_3OH on the Ir(221) surface

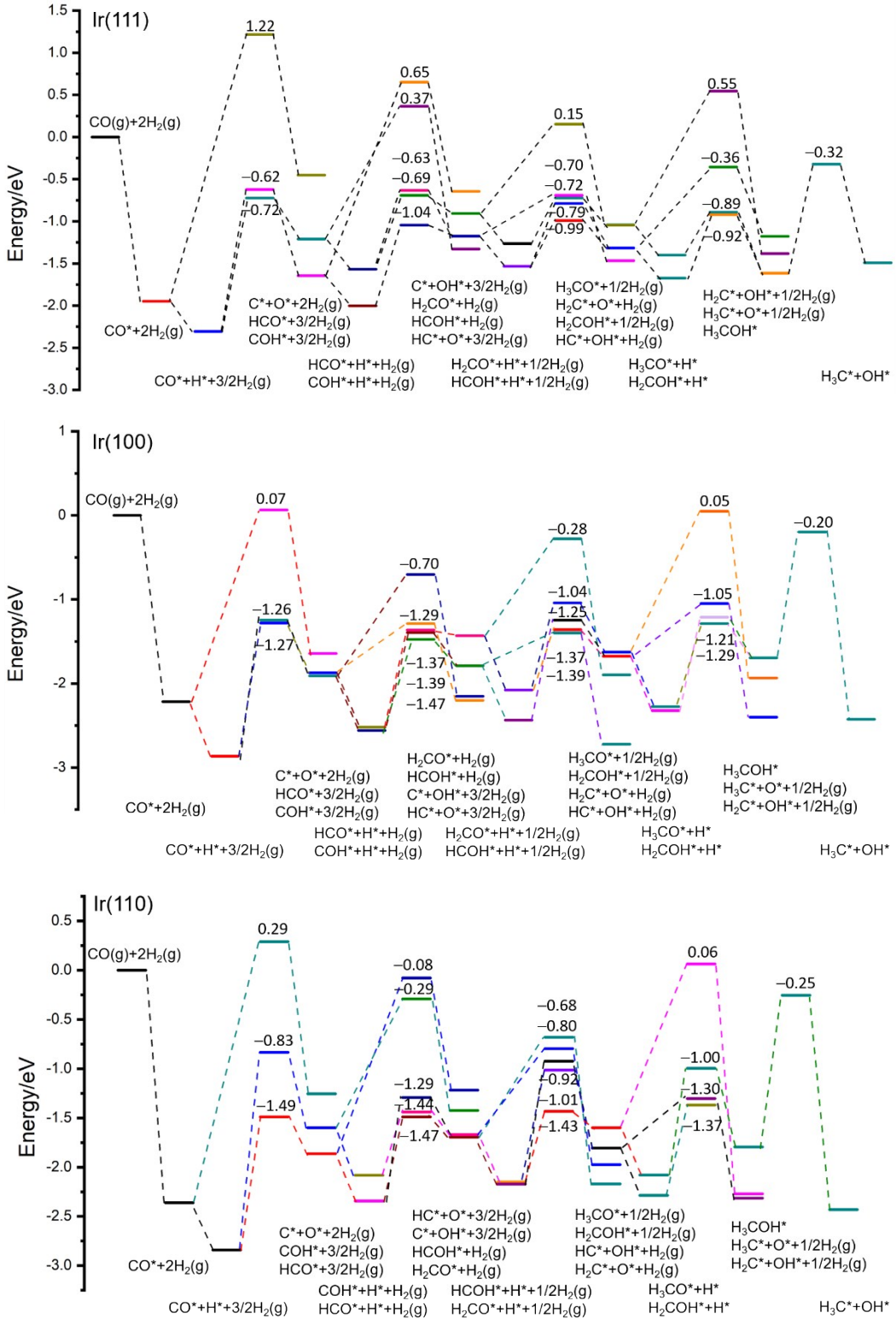
Ir(111)
Energy/eV
CO(g)+2H2(g)
CO*+2H2(g)
CO*+H*+3/2H2(g)
C*+O*+2H2(g)
HCO*+3/2H2(g)
COH*+3/2H2(g)
HCO*+H*+H2(g)
COH*+H*+H2(g)
C*+OH*+3/2H2(g)
H2CO*+H2(g)
HCOH*+H2(g)
HC*+O*+3/2H2(g)
H2CO*+H*+1/2H2(g)
HCOH*+H*+1/2H2(g)
H3CO*+1/2H2(g)
H2C*+O*+H2(g)
H2COH*+1/2H2(g)
HC*+OH*+H2(g)
H3CO*+H*
H2COH*+H*
H2C*+OH*+1/2H2(g)
H3C*+O*+1/2H2(g)
H3COH*
H3C*+OH*
Ir(100)
Energy/eV
CO(g)+2H2(g)
CO*+2H2(g)
CO*+H*+3/2H2(g)
C*+O*+2H2(g)
HCO*+3/2H2(g)
COH*+3/2H2(g)
HCO*+H*+H2(g)
COH*+H*+H2(g)
H2CO*+H2(g)
HCOH*+H2(g)
C*+OH*+3/2H2(g)
HC*+O*+3/2H2(g)
H2CO*+H*+1/2H2(g)
HCOH*+H*+1/2H2(g)
H3CO*+1/2H2(g)
H2COH*+1/2H2(g)
H2C*+O*+H2(g)
HC*+OH*+H2(g)
H3CO*+H*
H2COH*+H*
H3COH*
H3C*+O*+1/2H2(g)
H2C*+OH*+1/2H2(g)
H3C*+OH*
Ir(110)
Energy/eV
CO(g)+2H2(g)
CO*+2H2(g)
CO*+H*+3/2H2(g)
C*+O*+2H2(g)
COH*+3/2H2(g)
HCO*+3/2H2(g)
COH*+H*+H2(g)
HCO*+H*+H2(g)
HC*+O*+3/2H2(g)
C*+OH*+3/2H2(g)
HCOH*+H2(g)
H2CO*+H2(g)
HCOH*+H*+1/2H2(g)
H2CO*+H*+1/2H2(g)
H3CO*+1/2H2(g)
H2COH*+1/2H2(g)
HC*+OH*+H2(g)
H2C*+O*+H2(g)
H3CO*+H*
H2COH*+H*
H3COH*
H3C*+O*+1/2H2(g)
H2C*+OH*+1/2H2(g)
H3C*+OH*

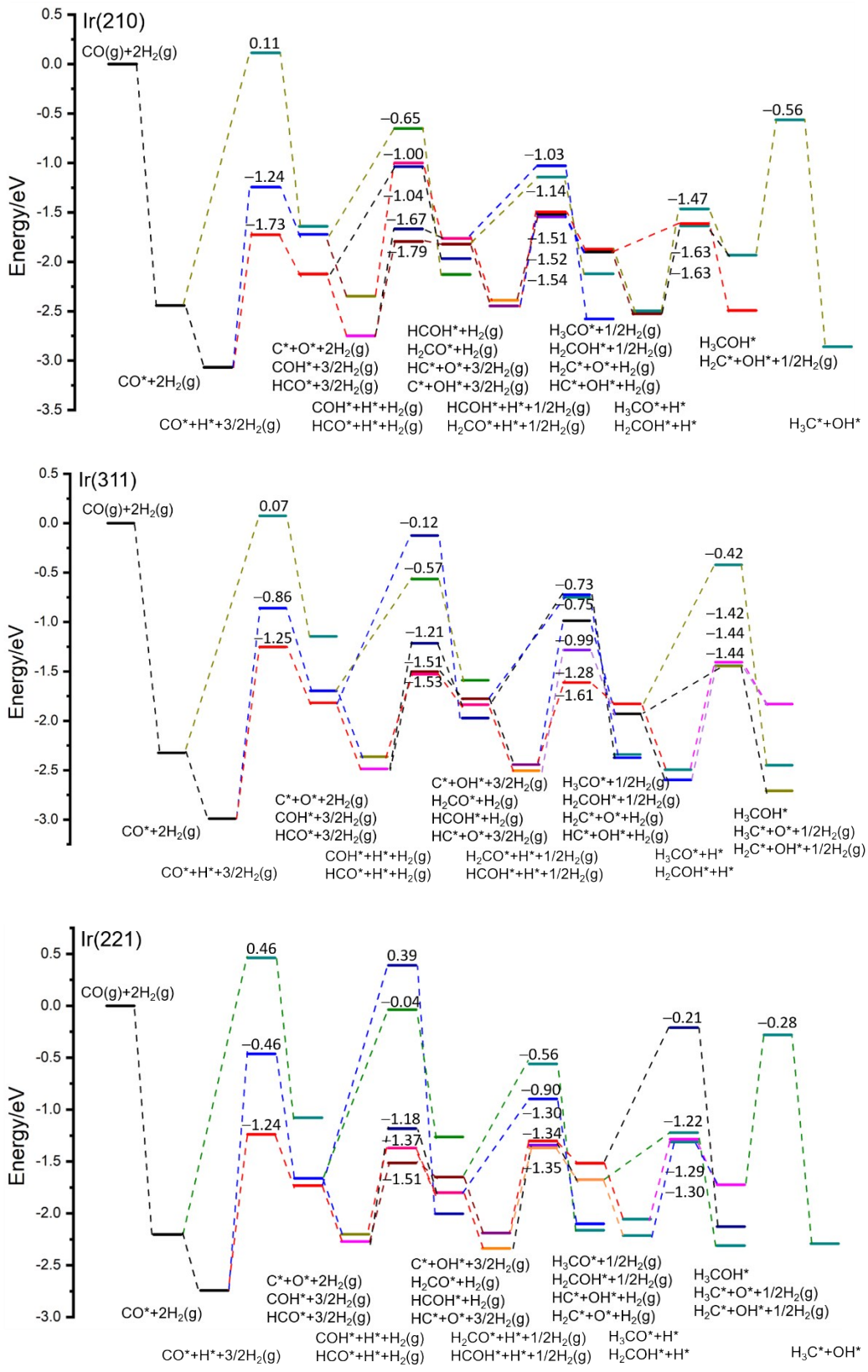

Figure S9 Surfaces of reaction potential energy of H-assisted CO dissociation on these six Ir surfaces

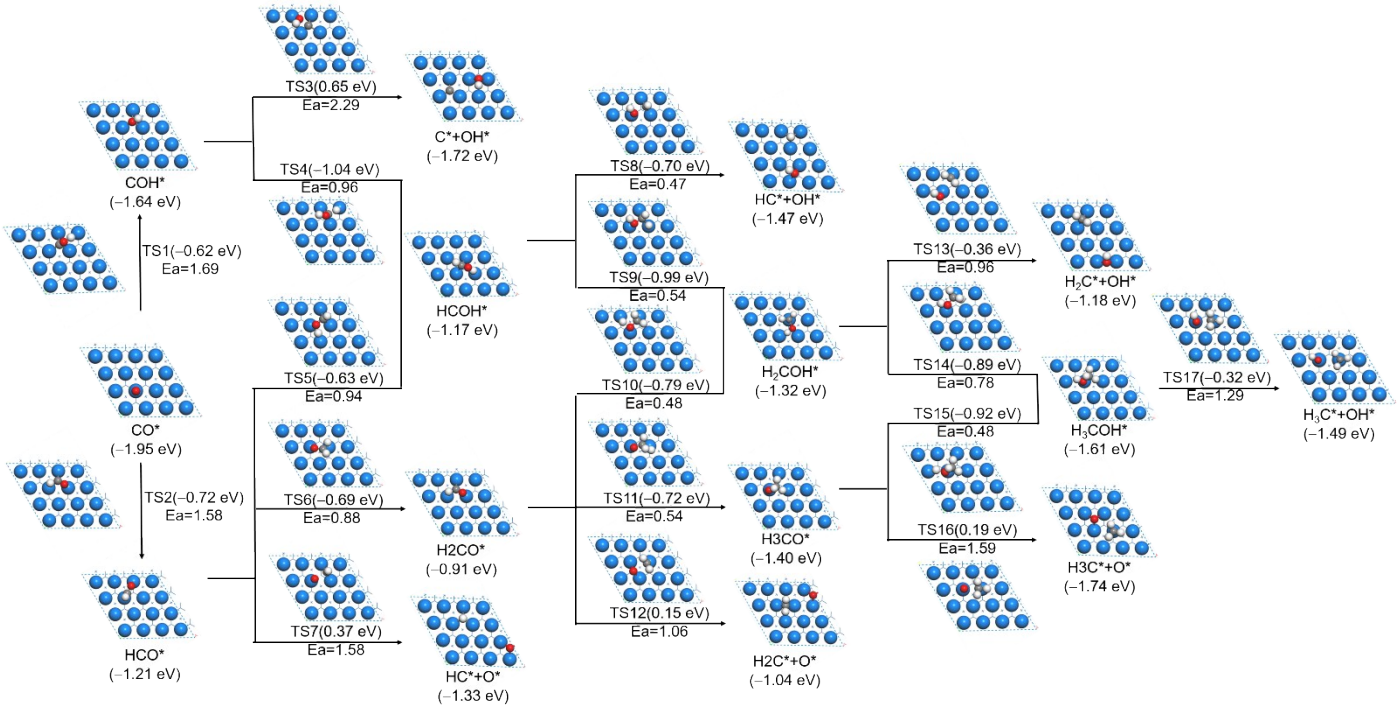

Figure S10 The progress of H-assisted CO dissociation, including the energies and structure parameters on the Ir(111) surfaces

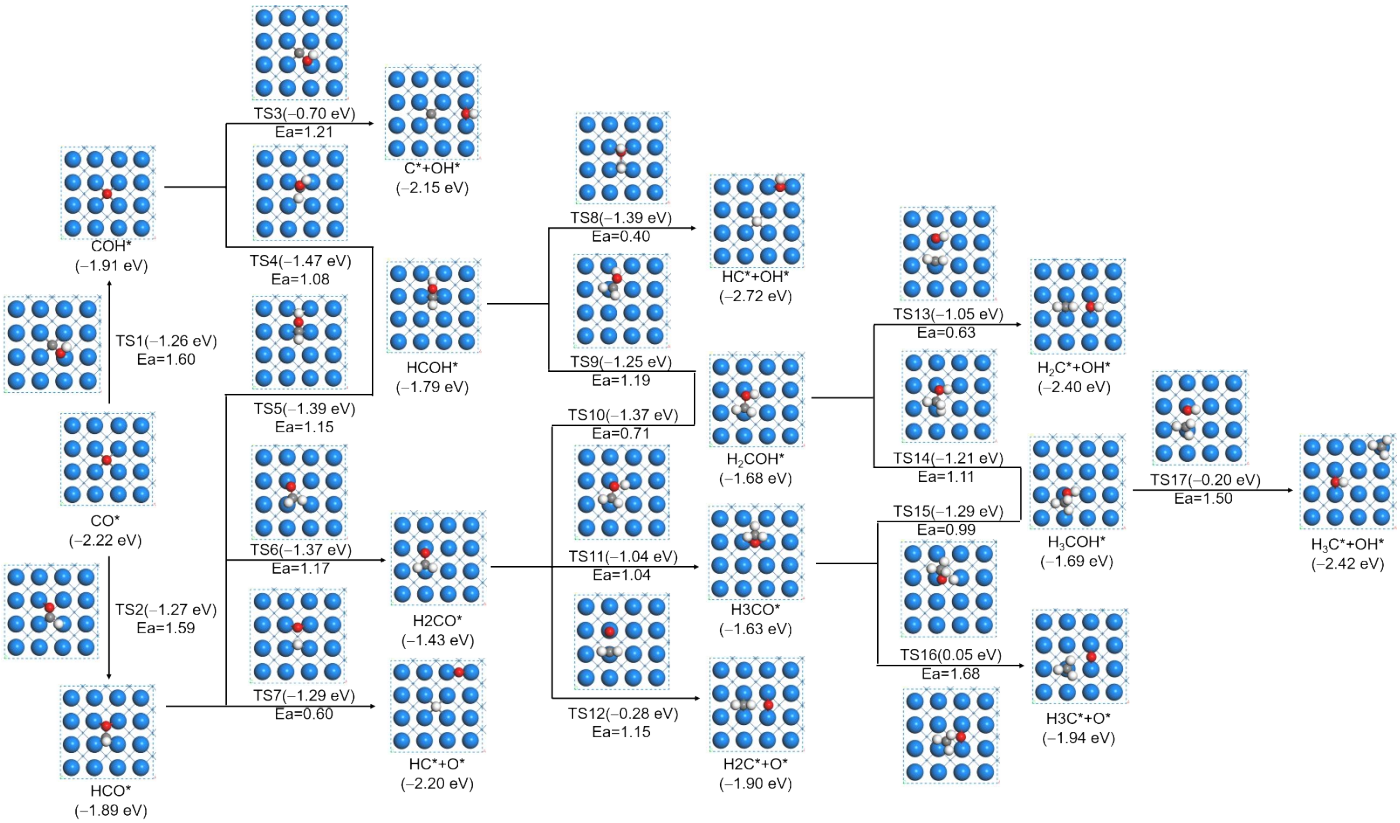

Figure S11 The progress of H-assisted CO dissociation, including the energies and structure parameters on the Ir(100) surfaces

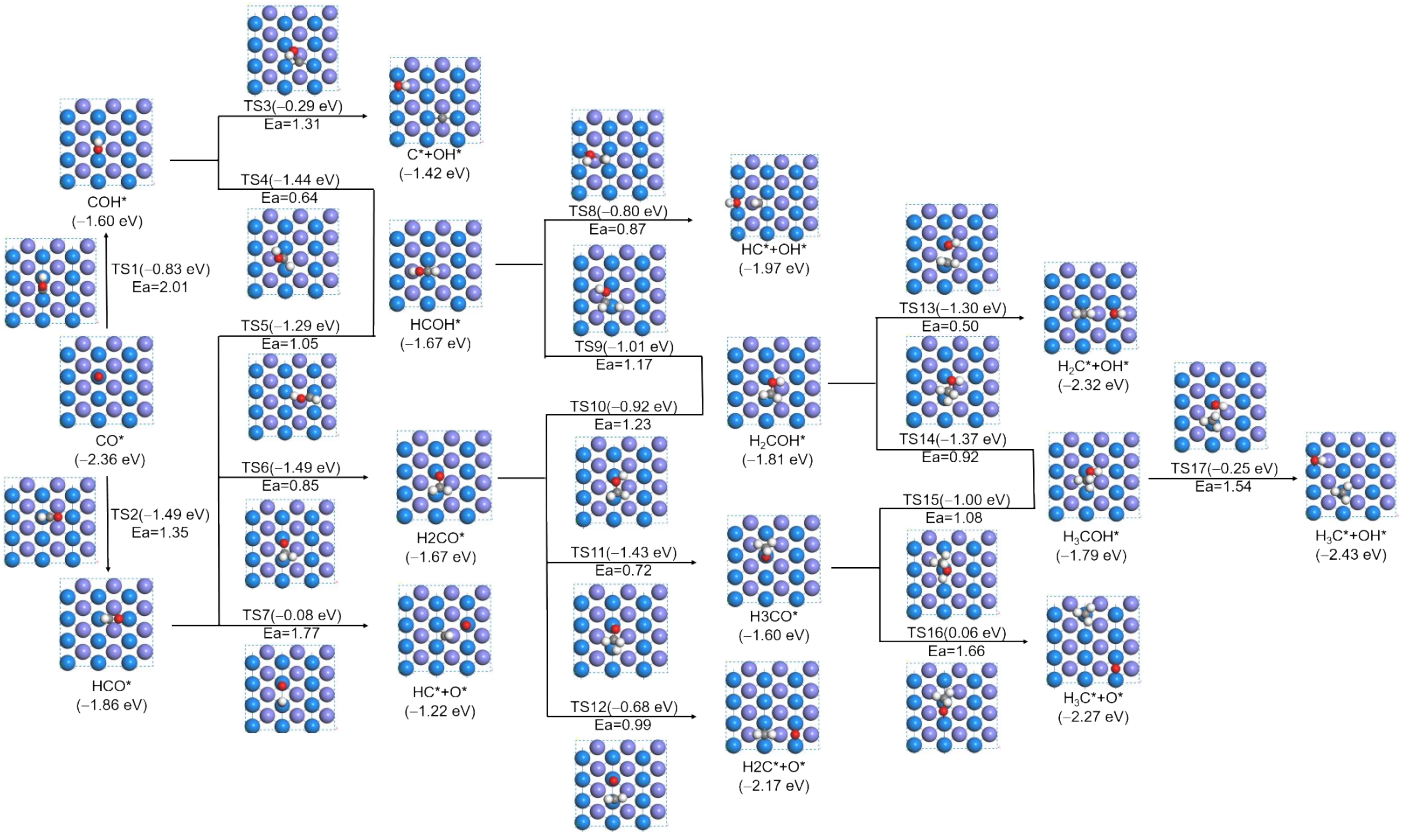

Figure S12 The progress of H-assisted CO dissociation, including the energies and structure parameters on the Ir(110) surfaces

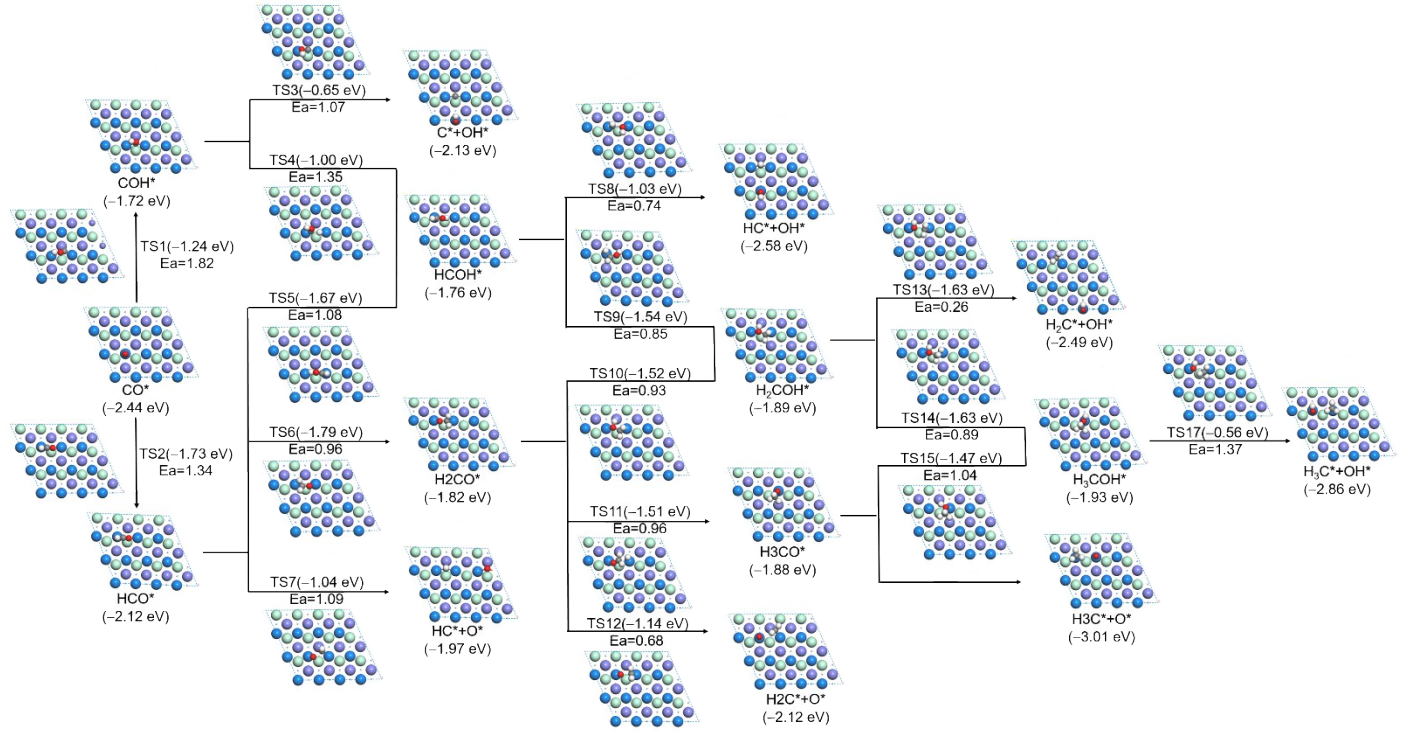

Figure S13 The progress of H-assisted CO dissociation, including the energies and structure parameters on the Ir(210) surfaces

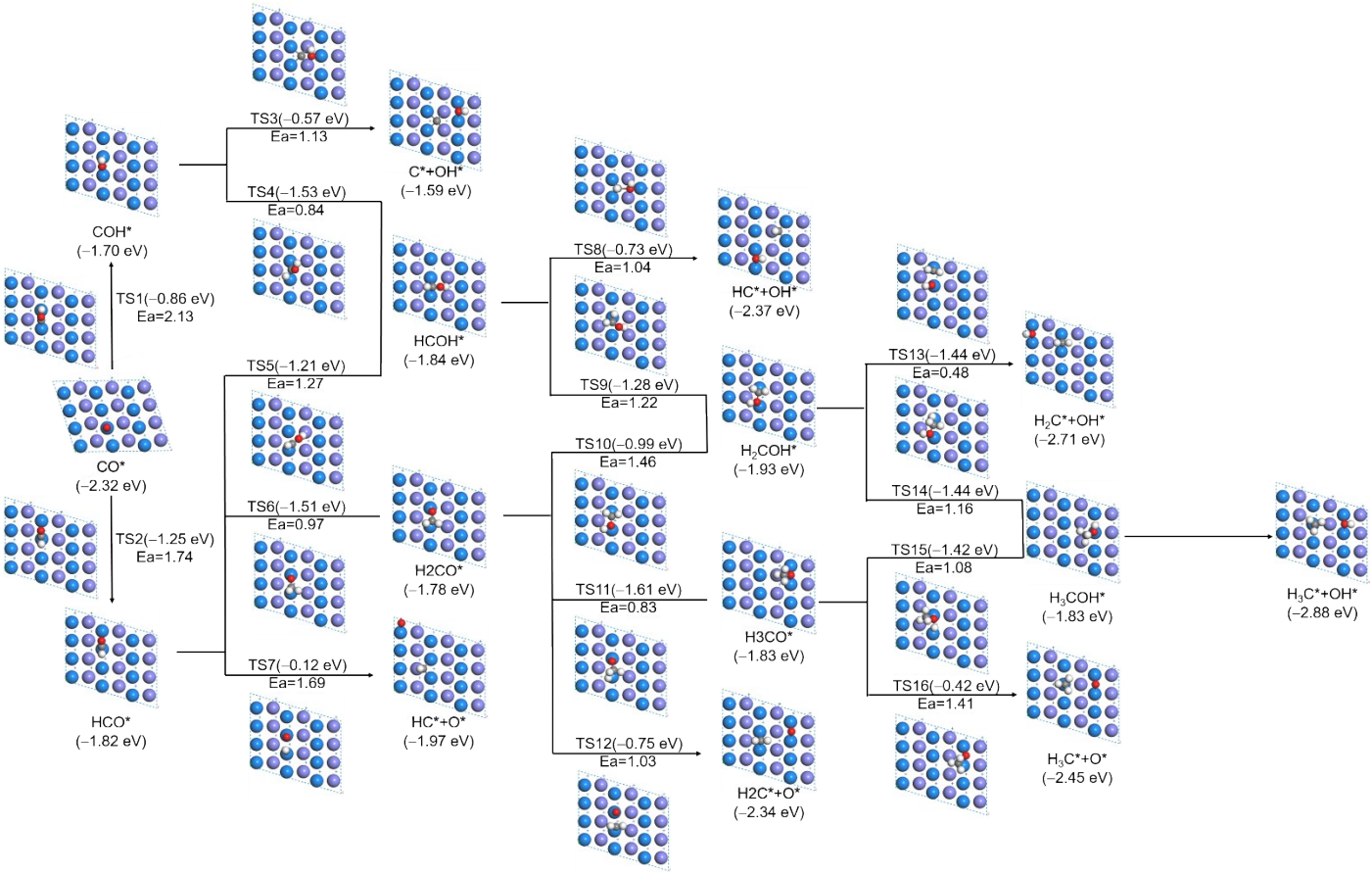

Figure S14 The progress of H-assisted CO dissociation, including the energies and structure parameters on the Ir(311) surfaces

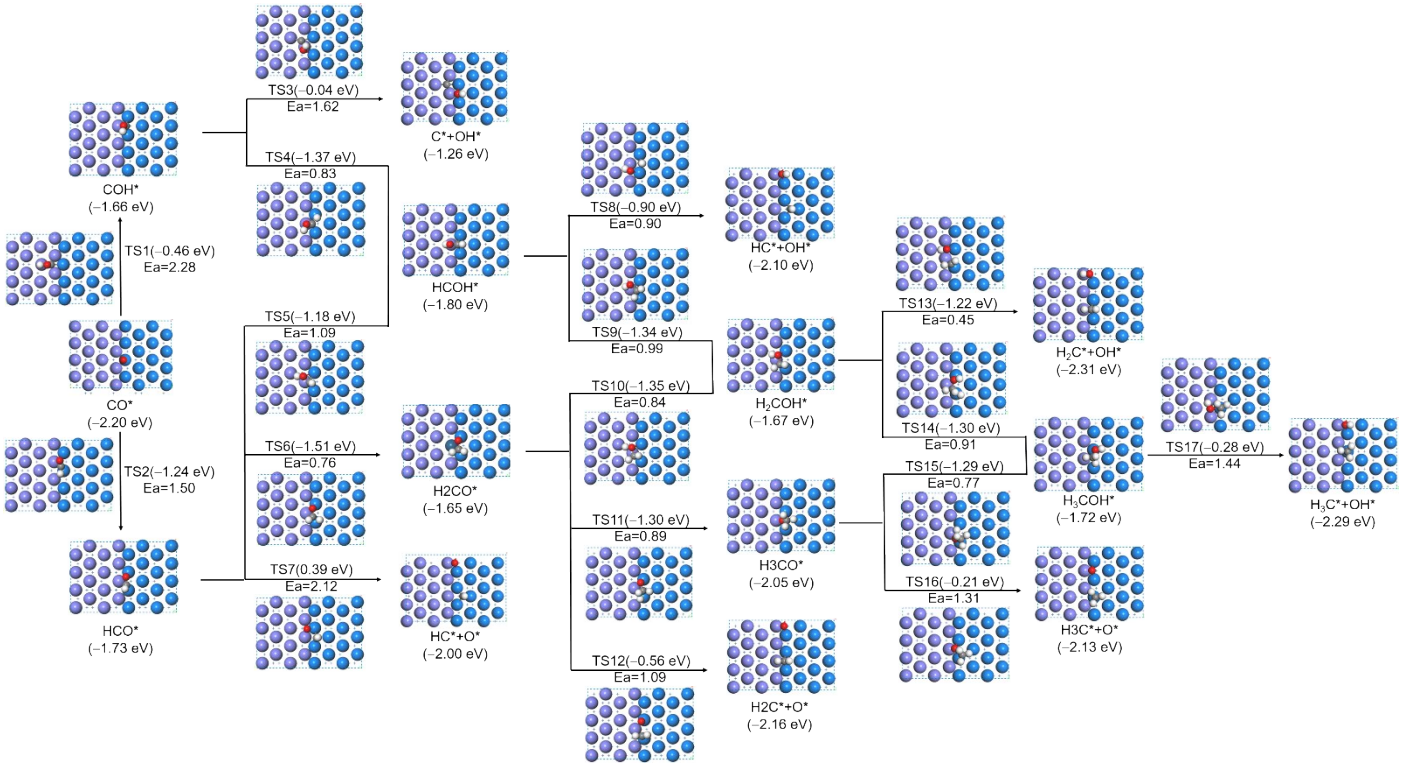

Figure S15 The progress of H-assisted CO dissociation, including the energies and structure parameters on the Ir(221) surfaces

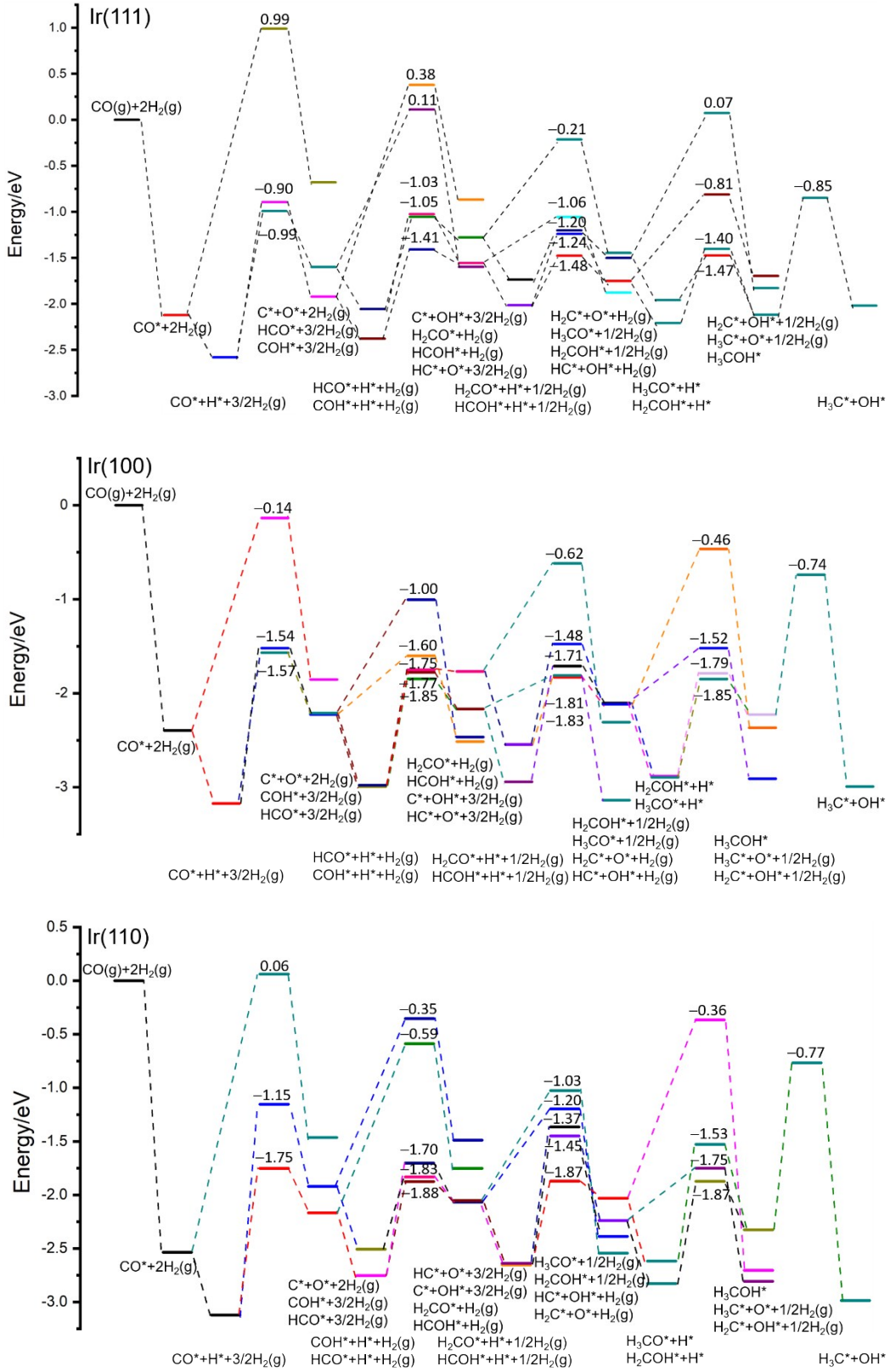
Ir(111)
Energy/eV
CO(g)+2H2(g)
CO*+2H2(g)
CO*+H*+3/2H2(g)
C*+O*+2H2(g)
HCO*+3/2H2(g)
COH*+3/2H2(g)
HCO*+H*+H2(g)
COH*+H*+H2(g)
C*+OH*+3/2H2(g)
H2CO*+H2(g)
HCOH*+H2(g)
HC*+O*+3/2H2(g)
H2CO*+H*+1/2H2(g)
HCOH*+H*+1/2H2(g)
H2C*+O*+H2(g)
H3CO*+1/2H2(g)
H2COH*+1/2H2(g)
HC*+OH*+H2(g)
H3CO*+H*
H2COH*+H*
H2C*+OH*+1/2H2(g)
H3C*+O*+1/2H2(g)
H3COH*
H3C*+OH*
0.99
−0.90
−0.99
0.38
0.11
−1.03
−1.05
−1.41
−0.21
−1.06
−1.20
−1.24
−1.48
0.07
−0.81
−1.40
−1.47
−0.85
Ir(100)
Energy/eV
CO(g)+2H2(g)
CO*+2H2(g)
CO*+H*+3/2H2(g)
C*+O*+2H2(g)
COH*+3/2H2(g)
HCO*+3/2H2(g)
HCO*+H*+H2(g)
COH*+H*+H2(g)
H2CO*+H2(g)
HCOH*+H2(g)
C*+OH*+3/2H2(g)
HC*+O*+3/2H2(g)
H2CO*+H*+1/2H2(g)
HCOH*+H*+1/2H2(g)
H2COH*+1/2H2(g)
H3CO*+1/2H2(g)
H2C*+O*+H2(g)
HC*+OH*+H2(g)
H2COH*+H*
H3CO*+H*
H3COH*
H3C*+O*+1/2H2(g)
H2C*+OH*+1/2H2(g)
H3C*+OH*
−0.14
−1.54
−1.57
−1.00
−1.60
−1.75
−1.77
−1.85
−0.62
−1.48
+1.71
−1.81
−1.83
−0.46
−1.52
−1.79
−1.85
−0.74
Ir(110)
Energy/eV
CO(g)+2H2(g)
CO*+2H2(g)
CO*+H*+3/2H2(g)
C*+O*+2H2(g)
COH*+3/2H2(g)
HCO*+3/2H2(g)
COH*+H*+H2(g)
HCO*+H*+H2(g)
HC*+O*+3/2H2(g)
C*+OH*+3/2H2(g)
H2CO*+H2(g)
HCOH*+H2(g)
H2CO*+H*+1/2H2(g)
HCOH*+H*+1/2H2(g)
H3CO*+1/2H2(g)
H2COH*+1/2H2(g)
HC*+OH*+H2(g)
H2C*+O*+H2(g)
H3CO*+H*
H2COH*+H*
H3COH*
H3C*+O*+1/2H2(g)
H2C*+OH*+1/2H2(g)
H3C*+OH*
0.06
−1.15
−1.75
−0.35
−0.59
−1.70
−1.83
−1.88
−1.03
−1.20
−1.37
−1.45
−1.87
−0.36
−1.53
−1.75
−1.87
−0.77

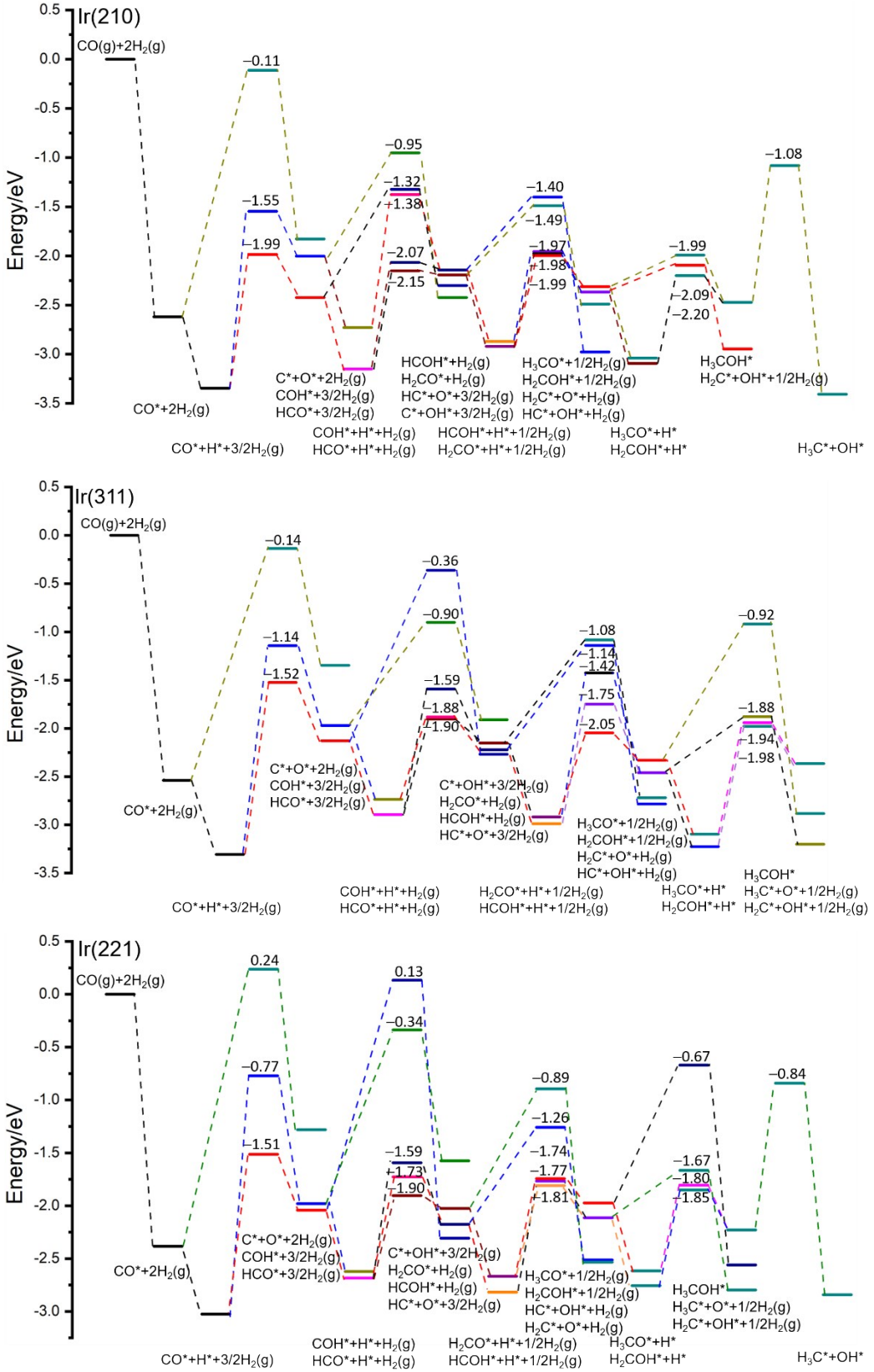

Figure S16 Gibbs free energy PES of H-assisted CO dissociation on these six Ir surfaces on the surfaces

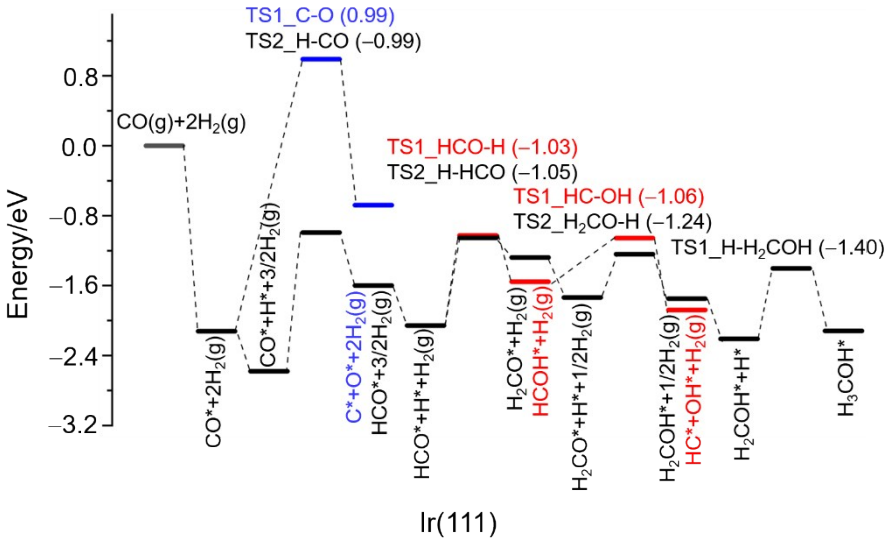
TS1_C-O (0.99)
TS2_H-CO (–0.99)
TS1_HCO-H (–1.03)
TS2_H-HCO (–1.05)
TS1_HC-OH (–1.06)
TS2_H2CO-H (–1.24)
TS1_H-H2COH (–1.40)
Energy/eV
0.8
0.0
–0.8
–1.6
–2.4
–3.2
CO(g)+2H2(g)
CO*+2H2(g)
CO*+H*+3/2H2(g)
C*+O*+2H2(g)
HCO*+3/2H2(g)
HCO*+H*+H2(g)
H2CO*+H2(g)
HCOH*+H2(g)
H2CO*+H*+1/2H2(g)
H2COH*+1/2H2(g)
HC*+OH*+H2(g)
H2COH*+H*
H3COH*
Ir(111)

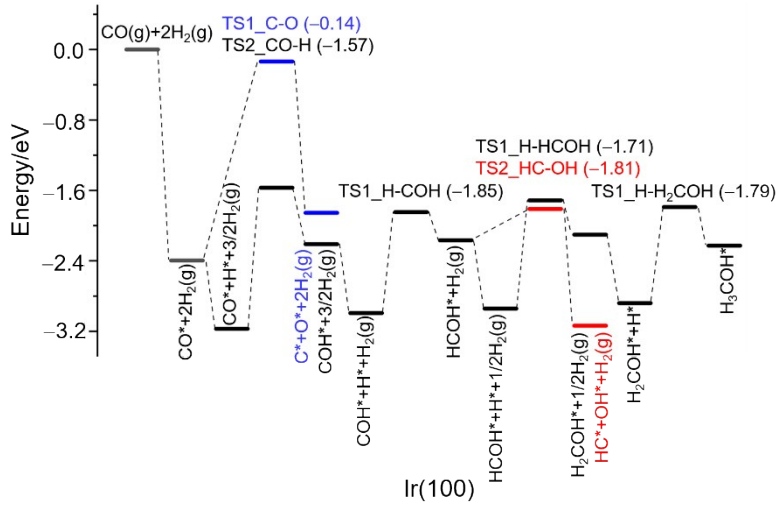
CO(g)+2H2(g)
TS1_C-O (–0.14)
TS2_CO-H (–1.57)
TS1_H-HCOH (–1.71)
TS2_HC-OH (–1.81)
TS1_H-COH (–1.85)
TS1_H-H2COH (–1.79)
Energy/eV
0.0
–0.8
–1.6
–2.4
–3.2
CO*+2H2(g)
CO*+H*+3/2H2(g)
C*+O*+2H2(g)
COH*+3/2H2(g)
COH*+H*+H2(g)
HCOH*+H2(g)
HCOH*+H*+1/2H2(g)
H2COH*+1/2H2(g)
HC*+OH*+H2(g)
H2COH*+H*
H3COH*
Ir(100)

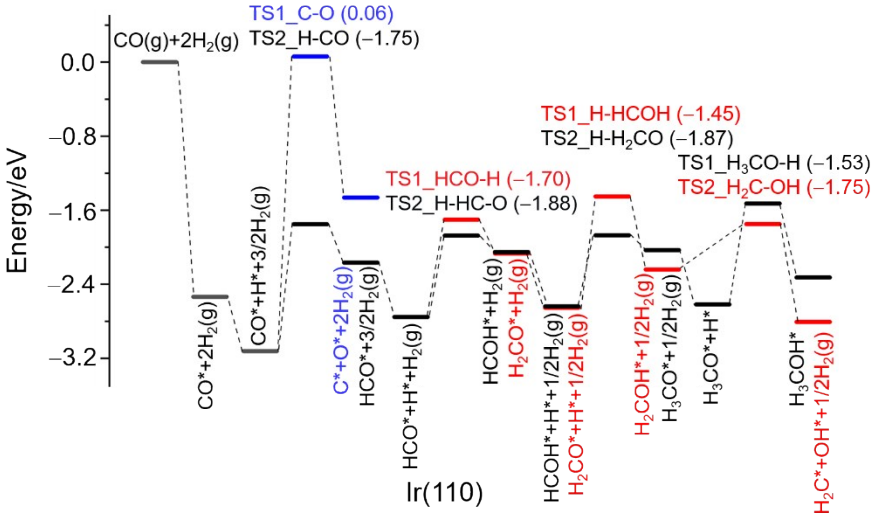
CO(g)+2H2(g)
TS1_C-O (0.06)
TS2_H-CO (–1.75)
TS1_H-HCOH (–1.45)
TS2_H-H2CO (–1.87)
TS1_H3CO-H (–1.53)
TS2_H2C-OH (–1.75)
TS1_HCO-H (–1.70)
TS2_H-HC-O (–1.88)
Energy/eV
0.0
–0.8
–1.6
–2.4
–3.2
CO*+2H2(g)
CO*+H*+3/2H2(g)
C*+O*+2H2(g)
HCO*+3/2H2(g)
HCO*+H*+H2(g)
HCOH*+H2(g)
H2CO*+H2(g)
HCOH*+H*+1/2H2(g)
H2CO*+H*+1/2H2(g)
H2COH*+1/2H2(g)
H3CO*+1/2H2(g)
H3CO*+H*
H3COH*
H2C*+OH*+1/2H2(g)
Ir(110)

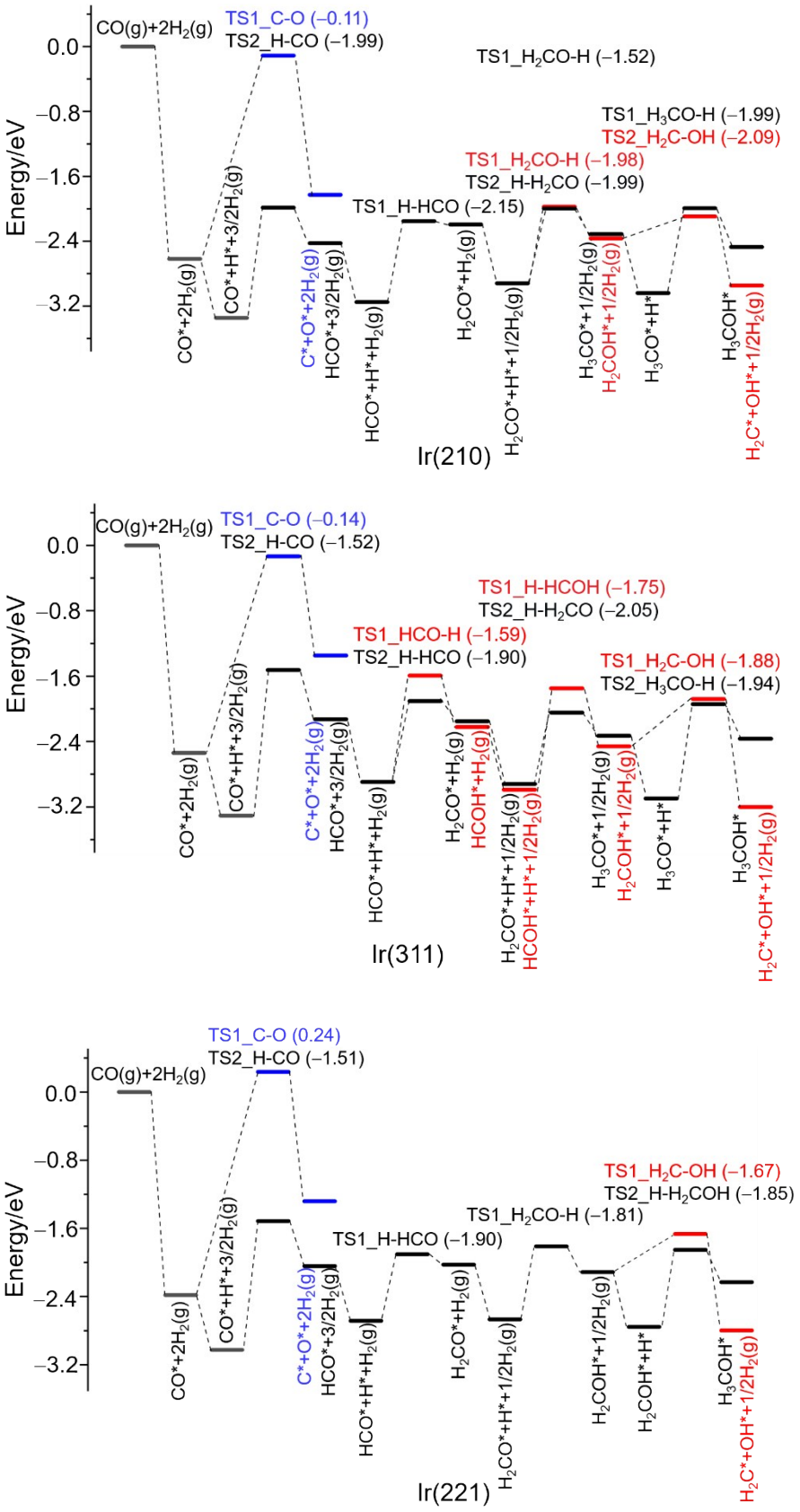

Figure S17 Gibbs free energy PES of the minimum energy path of H-assisted CO dissociation and methanol formation on these six Ir surfaces

REFERENCE

[1] L. Pauling, *J. Am. Chem. Soc.,* 1947, **69**, 542−553.

[2] N. E. Brese and M. O'Keeffe, *Acta Cryst. B,* 1991, **47**, 192−197.

[3] Y. He, P. Zhao, Y. Meng, W. Guo, Y. Yang, Y.-W. Li, C. Huo and X. Wen, *J. Phys. Chem. C*, 2018, **122**, 2806−2814.

[4] J. Yin, Y. He, X. Liu, X. Zhou, C. Huo, W. Guo, Q. Peng, Y. Yang, H. Jiao, Y.-W. Li and X. Wen, *J. Catal*., 2019, **372**, 217–225.

[5] I. D. Brown, *Chem. Rev.,* 2009, **109**, 6858–6919.

[6] I.D. Brown, http://www.ccp14.ac.uk/ccp/web2mirrors/I_d_brown/bond_valence_parm

[7] Z. Yao, C. Guo, Y. Mao and P. Hu, *ACS Catal.*, 2019, **9**, 5957−5973.